Physical Sensors: Radiation Sensors

Douglas S. McGregor and J. Kenneth Shultis

Kansas State University, Mech. and Nuclear Engineering, Manhattan, KS 66506
mcgregor@ksu.edu, jks@ksu.edu

Abstract

Ionizing radiation is detected primarily by sensing the presence of liberated free charges in a control medium. The medium may be a gas, liquid, or solid with electrodes positioned about the control volume. Summarized in this article are brief descriptions of the more common ionizing radiations encountered in the environment and the nuclear industry, along with the more common methods used to detect these radiations. Radiation detectors described include gas-filled, scintillation, and semiconductor devices. A brief section is included on radiation counting statistics.

Keywords:

Radiation, Radiation Detection, Radiation Measurement, Radiation Detectors

1 Types of Ionizing Radiation

Radiation is the emission of energy from a source, be it natural or stimulated. Although there are many types of radiation, this section is concerned mainly with the detection of *ionizing radiation*, consisting of energetic emissions of particles capable of producing (directly or indirectly) ionization in a substance. Typically, they are classified as charged-particle, electromagnetic, or neutral radiations.

1.1 Charged Particles

Alpha Particles Alpha particles were discovered in 1899 by Sir Ernest Rutherford who observed emissions from a uranium sample with an electroscope (Rutherford, 1899). He deduced that at least two types of particles were emitted from the samples, one easily stopped with aluminum sheets which he called alpha radiation and the other significantly more penetrating which he named beta radiation.

Alpha particles, denoted by the Greek letter 'α', are doubly positive-charged particles composed of two neutrons and two protons. Although identical to helium nuclei, they are identified as particles emitted from the nucleus of an atom. By contrast, a helium atom stripped of its electrons in an accelerator is best described as a doubly-ionized helium nucleus and not an α particle.

Alpha particles, with a mass of about 4.01506 u (6.644657×10^{-27} kg), are highly ionizing. Alpha particles are emitted from nuclei with distinctive discrete energies, which enable spectroscopic identification of α-particle emitting radioisotopes. Ranges in matter vary, but are generally short because of the high stopping power ($-dE/dx$) in materials, varying from a few centimeters in gases at 1 atm pressure to a few tens of microns in solids and liquids. Detection methods usually rely on sensing the free ionization produced in the detecting medium.

Beta Particles, Positrons, Electrons, Auger Electrons, Conversion Electrons Beta particles, also discovered in 1899 by Sir Ernest Rutherford along with α particles, were found to be generally more penetrating than α radiation. By using the method developed by J.J. Thomson to measure the mass-to-charge (m/q) ratio for electrons (Thomson, 1897), beta particles, denoted by the Greek letter 'β,' or more precisely 'β^-', were shown by Antoine Henri Becquerel to be fast moving electrons emitted from the nucleus of an atom (Becquerel, 1900). With a rest mass of 9.10938×10^{-31} kg, a β^- particle is an electron emitted in radioactive decay of a nucleus and is accompanied by simultaneous emission of an antineutrino emission. Consequently, β^- particles are emitted with a continuum of energies between zero and the Q-value of the decay reaction.

A *conversion electron* is produced when an excited nucleus transfers its excitation energy to an orbital electron, usually in the K shell, thereby, ejecting it from the atom. This process is referred to as *internal conversion*. An Auger electron is similar, but is caused by an orbital electron dropping into a lower vacant electron state. The energy difference between the two states is either emitted as an x ray (fluorescence) or transferred to an outer orbital electron, thereby, ejecting it from the atom as an Auger electron. Conversion electrons and Auger electrons are emitted with discrete energies.

A *positron* is an antielectron, with the same rest mass and spin but opposite charge of an electron, and is emitted in a β^+ radioactive decay, together with a neutrino, when a nuclear proton is transformed to a neutron through the weak force. They can also be produced in so-called *pair-production* photon interactions within the intense electric field near the nucleus of an atom if the photons have an energy exceeding $2m_ec^2 = 1.022$ MeV (Evans, 1955; Kaplan, 1962; Shultis and Faw, 2000). They can also be produced far less frequently in the electric field of an orbital electron in a reaction called *triplet production* if the incident photon has an energy above $4m_ec^2$ (Evans, 1955). Positrons usually quickly annihilate with ambient electrons after they lose their kinetic energy. The annihilation produces two opposite moving photons each with an energy of 511 keV. Although much less ionizing than α particles, i.e., they have a smaller collisional stopping power and therefore are more penetrating, detection of these electron-like particles mainly relies on sensing the free ionization they produced by interacting with ambient atoms in the detecting medium.

Fission Fragments and Products Fission fragments and fission products are often confused, but there is an important difference. Fragments are the particles released immediately after a fission (scission) occurs, usually resulting in the release of two, but sometimes three, *fission fragments*. These highly excited and highly ionized fragments of "nuclear fluid" are extremely unstable. They emit almost all fission neutrons within 10^{-14} s of the fission event and, through isomeric decay, the fragments emit several MeV of prompt gamma rays within the first 60 ns after a fission. For example, thermal-neutron induced fission of $^{235}_{92}$U with a Q-value of 202.5 MeV yields 8.13 ± 0.35 prompt gamma rays having an average total energy of 7.25 ± 0.26 MeV per fission, distributed over a continuum of energies between 0.1 to 10.5 MeV (Shultis and Faw, 2000). On average, prompt neutrons have about 4.9 MeV, while the combined fission fragments have about 169 MeV. The remaining energy is divided between β^-, neutrino, and delayed γ radiation. After prompt-neutron and gamma-ray emission, the still highly ionized fast-moving fragments rapidly slow because of their high collisional stopping power $-dE/dx$. During the slowing process they capture ambient electrons to become neutral *fission products* which then undergo β^- decay over the next several hundred years through a chain of radioactive daughters. Notably, there are seven fission products with half-lives greater than 10^5 years. As with other charged particles, ionization within the detector medium is commonly used for fission fragment detection, although other detection methods do exist.

1.2 Electromagnetic Radiation

Different types of ionizing electromagnetic radiation are are defined by the mechanism of its origin and not by the energy of its photons. The energetic photons of the different types of electromagnetic radiation are generally detected by similar means regardless of their origin. The principal interactions used for photon detection are the photoelectric effect, the Compton scattering effect, and the pair production effect. These effects produce, either directly or indirectly, energetic charged particles, which, in turn, create additional charge carriers through Coulombic interactions with the ambient medium. Usually photons are detected by sensing the presence of the charge carriers, although other techniques can be used.

X Rays X rays were discovered by Wilhelm Röntgen in 1895 while he was conducting experiments with a Crookes tube (Röntgen, 1895; 1896), a type of cathode-ray tube. While in a darkened room, he noticed a plate, coated with a scintillating mixture of platino-barium-cyanide ($BaPt(CN)_4$), would glow when the

Crookes tube was activated. This led to his conclusion that invisible rays were emanating from the Crookes tube and were causing the glowing effect.

Although x-ray photons generally have lower energies than those of most gamma rays, it is incorrect to differentiate between x rays and gamma rays by their energy. X rays are ionizing photons produced when a charged particle, such as an electron, undergoes a reduction in energy either by electronic transitions from an atomic orbital to a lower energy orbital or by interactions with a strong electromagnetic field. By contrast, gamma rays are released by the transitions of a nucleon from an excited state in the nucleus to a lower energy state.

Characteristic x rays are released with discrete energies by electronic transitions from higher to lower atomic orbital energy states. They are categorized by the initial and final electronic shells (orbitals). For instance, an electron dropping from the L shell to the K shell yields a K_α x ray and from the M shell to the K shell yields a K_β x ray. Transitions from an outer shell down to the L shell are L x rays, where M to L yields an L_α x ray and a N to L generates an L_β x ray.

Bremsstrahlung x rays ("breaking radiation") are emitted over a continuous spectrum as fast electrons (or beta particles) centripetally decelerate in the strong electric field near the nucleus of an ambient atom. The endpoint energy of the emitted continuous photon spectrum is the initial energy of the electron when it enters the slowing medium. However, the most probable x-ray energy is usually substantially less than this maximum energy. It is bremsstrahlung radiation, usually accompanied by characteristic x rays, that is emitted from common x-ray tubes. Bremsstrahlung can also be emitted by any charged particle, but electron generated bremsstrahlung is usually of most concern.

Sychrotron/Cyclotron x rays, also known as *magnetobremsstralung*, are produced by *accelerating* charged particles, usually from interactions with a strong magnetic field such as those encountered in particle accelerators or active astronomical objects such as pulsars and black holes.

Gamma Rays Gamma rays (γ rays) were discovered by Paul Villard in 1900 while conducting experiments with a radium source and photographic film (Villard 1900a; 1900b). Within a strong magnetic field, he noticed that three visible areas were produced on a photographic plate. One radiation type was easily blocked by a thin shield and was also deflected as positive particles (α particles), one type was deflected as negative particles (β^- particles), and a third type was not deflected at all and was also highly penetrating. Villard did not name this newly discovered radiation, but instead it was Ernest Rutherford who offered the name "γ radiation" in sequence with α and β radiation.

A gamma ray is electromagnetic ionizing radiation emitted from an atomic nucleus transitioning from an excited state to a lower energy state. Gamma rays can be highly penetrating and their detection is improved by using detectors constructed from relatively high atomic number materials and large detector volumes.

Annihilation Photons Annihilation photons are also identified by their origin, namely, the destructive joining of a subatomic particle to its antiparticle. For practical detection purposes, the most common annihilation photons encountered are 511-keV photons emitted from the combination of an electron with a positron. The 511-keV energy is the rest mass energy equivalent of an electron (or positron). Usually annihilation occurs after an initially fast moving β^+ particle has completely slowed before annihilating with an ambient electron so, consequently, the two 511-keV annihilation photons are emitted in opposite directions to preserve the zero linear momentum condition. However, so-called in-flight annihilation does occur. There are certainly more complicated annihilation schemes, such as found with baryon-antibaryon reactions and neutrino-antineutrino reactions, yet these reactions can be quite involved and generally beyond the scope of the present article on radiation detection.

1.3 Neutral Particles

Neutrons Neutrons were discovered by James Chadwick in 1932, who received the 1935 Nobel Prize in Physics for this discovery (Chadwick, 1932). Neutrons are subatomic particles with zero charge and mass of 1.674927×10^{-27} kg, slightly more than that of a proton. A neutron is composed of two down quarks and one up quark. Neutrons are fundamental baryon particles that make up atomic nuclei, the others being protons (1.672621×10^{-27} kg). Although neutrons have no electronic charge, they can still cause ionization in a medium through absorption or scattering reactions.

Neutrinos and Anti-Neutrinos A neutrino is a subatomic particle with mass much smaller than other elementary particles. It has spin of 1/2 with a net neutral charge. They are weakly interacting particles and usually pass through material without interacting. The anti-neutrino is similar to the neutrino, also neutral, but with opposite lepton number and chirality. There are three types of neutrinos: the electron neutrino, the muon neutrino, and the tauon neutrino which oscillate from one form to another as they travel. Electron antineutrinos are emitted in beta-particle radioactive decay. Massive detectors are required for neutrino detection, often taking advantage of the Ĉerenkov radiation effect in transparent materials (water, heavy water, etc.).

2 Gas-Filled Detectors

In 1908, Ernest Rutherford and Hans Geiger constructed a device composed of a metallic cylinder containing a thin wire along the axis (Rutherford and Geiger, 1908). The gas medium in the device was air. Application of a voltage between the cylinder and wire produced sizable currents, measured with an electrometer, when α particles were directed into the cylinder. They also noticed that the behavior of the detector changed with increasing voltage. In particular, α particles could be detected at much lower applied voltages than could be β^- particles. This behavior and its application is referred to as *proportional* counting. Several distinct voltage regions of operation are clearly apparent in Fig. 1.

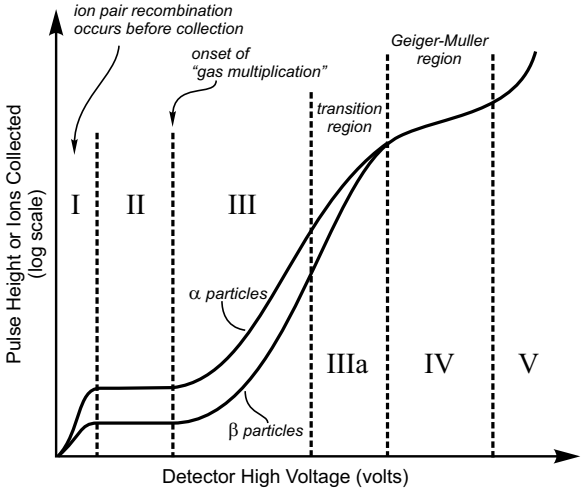

Figure 1. The observed output pulse height versus the applied high voltage for a gas-filled detector, showing the main regions: (I) recombination, (II) ion chamber, (III) proportional, (IV) Geiger-Müller, and (V) continuous discharge. This plot is often referred to as the *gas curve*. Copyright (2020). From Radiation Detection: Concepts, Methods and Devices by D.S. McGregor and J.K. Shultis. Reproduced by permission of Taylor and Francis Group, LLC, a division of Informa PLC.

Direct radiation interactions in the gas or particles ejected from the chamber walls by radiation interactions cause some of the detector gas to become ionized. Through a cascade of ionization from primary and secondary ionization, a charge cloud composed of electrons and positive ions appears. A voltage placed across electrodes in the gas chamber causes the electrons and ions to drift apart, where electrons drift towards the anode and the positive ions drift towards the cathode. As the *charge carriers* move through the chamber, they induce current to flow in a circuit externally connected to the chamber. This current, or change in current, can then be measured as an indication that a radiation interaction occurred in the chamber (Korff, 1946; Wilkinson, 1950).

2.1 General Operation

At low voltages in the *recombination region*, denoted as Region I of Fig. 1, some measurable current is seen although considerable recombination occurs. As the voltage is increased, electron-ion pair separation becomes more efficient until practically no recombination occurs. Hence, the measured current is indicative of the total number of electron-ion pairs formed. Negligible recombination occurs in Region II of Fig. 1 and is referred to as the *ionization chamber region*. As the voltage is increased further, the electrons gain enough kinetic energy to create more electron-ion pairs through impact ionization. This ionization provides a mechanism for signal gain, often referred to as *gas multiplication*. The observed current increases as the voltage increases, but still remains proportional to the energy of the original radiation particle. This voltage region is shown on the gas curve as Region III. Increasing the applied voltage further causes nonproportional current increases and is indicated as Region IIIa. At even higher electric fields, defined as region IV, all currents, regardless of origin, radiation species, or energies, have the same magnitude. This region is called the *Geiger-Müller region*. Finally, excessive voltage drives the detector into Region V where the voltage causes sporadic arcing and other spontaneous electron emissions to occur, hence causing *continuous discharging* in the detector. Gas detectors should not be operated in the continuous discharge region.

Gas detectors can be operated in *pulse mode* or *current mode*. Pulse mode is generally used in low to moderate radiation fields. For pulse mode, a single radiation quantum, such as an alpha particle, beta particle or gamma ray, interacts in the chamber volume and produces an ionized cloud. The charge carriers drift apart and they induce current to flow to the device terminals. A charging circuit, usually consisting of a preamplifier and feedback loop, integrates the current and stores the charge, thereby producing a voltage potential. This voltage is measured as a *single* event, indicating that a single radiation quantum has been detected. The preamplifier circuit is subsequently discharged and reset, allowing the device to measure the next radiation interaction event. Hence, each voltage pulse from the detector indicates an individual radiation interaction event. Although extremely useful, there are limitations to pulse mode operation. Should another radiation interaction occur while the detector is integrating or discharging the current from a previous interaction event, the device may not, and usually does not, record the new interaction, a condition referred to as *pulse pile up*. The time duration in which a new pulse can not be recorded is the detector *recovery time*, sometimes referred to as *dead time*.

For high radiation fields, gas detectors are operated in current mode, in which the radiation induced current is measured on a current meter. Under such conditions, many interactions can occur in the device in short periods of time, and the observed current increases as the radiation interaction rate in the chamber increases. Hence, current mode can be used to measure the intensity of high radiation fields; the magnitude of the current is a measure of the radiation-induced ionization rate in the detector, which, in turn, is a measure of the strength or intensity of the radiation field in which the device is being operated. The disadvantage of current mode operation is that individual radiation interactions can not be identified.

2.2 Ion Chambers

Ion chambers are operated in Region II of the gas curve (Fig. 1). Ion chambers come in many forms, and can be used for reactor power measurements, where the radiation field is very high, survey intruments in moderate radiation fields, and as small personnel dosimeters, for use where radiation levels are usually low. When ionizing radiation interactions occur in the gas, they produce electron-ion pairs relative in number to the radiation energy absorbed. The voltage applied across the electrodes causes the negative electrons to separate from the positive ions and drift across the chamber volume. Electrons drift towards the anode and positive ions drift towards the cathode, and their movement *induces* current to flow in the external circuit.

Two difficulties are encountered when operating ion chambers in the pulse mode: (1) the measured signal is small because the current is composed of only the primary (or initial) electron-ion pairs excited by the

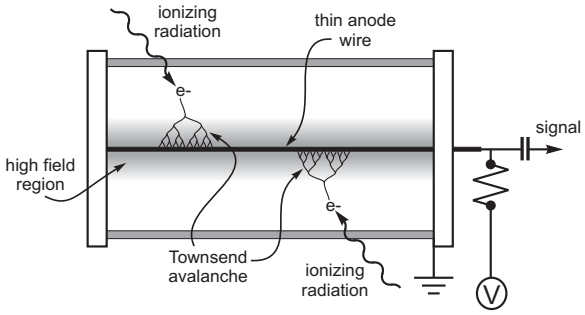

Figure 2. With a high electric field near the anode of a gas-filled detector, signal gain is realized through impact (Townsend) avalanching and is referred to as "gas multiplication". Copyright (2020). From Radiation Detection: Concepts, Methods and Devices by D.S. McGregor and J.K. Shultis. Reproduced by permission of Taylor and Francis Group, LLC, a division of Informa PLC.

radiation quantum and (2) the signal formation time can be long due to the slow motion of the heavy positive ions. Often, an RC circuit is connected to an ion chamber to reduce the time constant of the system and to discharge the capacitor *before* all of the ions are collected in order to reduce response time.

Ion chambers operated in the current mode are stable and have a long life. Large ion chambers are used as area monitors for ionizing radiation and high-pressure chambers offer a relatively high sensitivity, permitting measurement of exposure rates as low as 1 μR/h. At the other extreme, small chambers with low gas pressures can be operated in radiation fields with exposure rates as great as 10^7 R/h.

An ion chamber can be coated with a strongly-absorbing neutron-reactive material or filled with a neutron reactive gas, thereby making it sensitive to neutrons (Grosshoeg, 1979). Common isotopes for gas-filled neutron detectors are ^{3}He, ^{10}B, ^{6}Li, and ^{235}U. Neutron sensitive ion chambers can be filled with $^{10}BF_3$ or ^{3}He gas, or the inside walls of the chamber are coated with ^{10}B, ^{6}LiF, or ^{235}U. Ion chambers that use ^{235}U are often referred to as fission chambers, because it is the fission fragments from the fission of ^{235}U that ionize the chamber gas. These gas-filled neutron detectors can be operated as ion chambers or proportional counters. Because of pulse pile up, ion chambers and fission chambers are generally not operated in pulse mode when in high radiation fields.

2.3 Proportional Counters

At sufficiently high voltages, electrons can gain enough kinetic energy to cause additional ionization and excitation in the gas, an effect called *impact ionization*. These newly liberated electrons can also gain enough energy when accelerated by the electric field to cause even more ionization. The process continues until the electrons are collected at the anode. The entire process of generating the impact ionization cloud is called a *Townsend avalanche*, or sometimes *gas multiplication*, as illustrated in Fig. 2. There is a critical electric field E_A at which gas multiplication begins and below which the electrons do not gain sufficient energy to cause impact ionization. This threshold electric field defines the transition between Region II and Region III in the gas curve. Detector configurations of parallel plates, which can be used for ion chambers, are seldom used for proportional counters. A preferred geometry is either a coaxial configuration (depicted in Figs. 2 and 3) or a pseudo-hemispherical geometry. Pulse formation is dependent on the formation of a large electron-ion charge cloud near the anode. Consequently, it is the drift of the positive ions that induces most of the output signal. Approximately half of the maximum signal it formed as positive ions drift within the first mm of the anode wire towards to the cathode. The dead time is reduced by adjusting the RC time

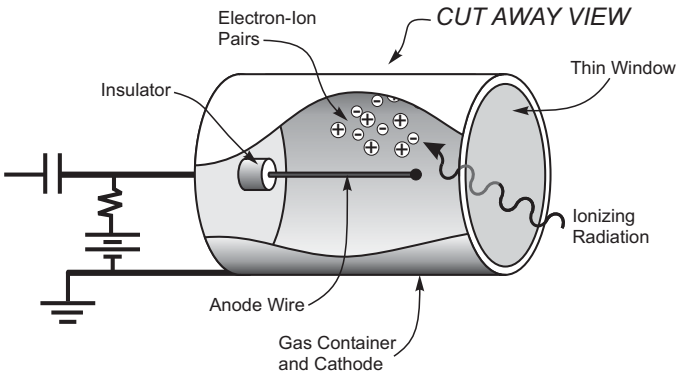

Figure 3. Schematic view of a coaxial gas detector, which is commonly used for Geiger-Müller tubes, and sometimes used for proportional counters. High voltage is applied to the central wire anode, while the outer cylinder wall, the cathode, is held at ground. Copyright (2020). From Radiation Detection: Concepts, Methods and Devices by D.S. McGregor and J.K. Shultis. Reproduced by permission of Taylor and Francis Group, LLC, a division of Informa PLC.

constant of the device with only minor effect on the overall performance. Dead times for typical proportional counters are on the order of tens of microseconds.

Continuous waves of avalanches can occur if ultraviolet (UV) light, released by the excited atoms or ions produced in one avalanche, ionize too many gas atoms after the initial ionization event. These gas ions, when arriving at the cathode wall, can strike with enough kinetic energy to cause the ejection of more electrons, causing another avalanche (Liebson, 1947; Sitar et al., 1993). To prevent continuous waves of avalanching from occurring in the chamber after a radiation interaction, a *quenching gas* is added to the gas mixture, typically a polyorganic molecule. A common proportional counter gas is P-10, which is a mixture of 90% Ar and 10% methane (the quenching gas). When an ionizing particle enters the detector, it ionizes both the Ar and the quenching gas. However, as the Ar gas ions drift through the chamber, they transfer their charge to the quench gas molecules. The quench gas ions continue to drift and carry the positive charge to the cathode wall. When a quench gas is struck by a UV photon or strikes the cathode wall, it dissociates by releasing a hydrogen atom rather than ejecting an electron. Hence, the quench gas prevents continuous waves of avalanches.

As with ion chambers, a neutron detector can be fashioned with a proportional counter by backfilling the chamber with a neutron reactive gas (usually ^{3}He or $^{10}BF_3$). Because such a device operates in proportional mode, a low resolution spectrum associated with the reaction product energies of either the ^{10}B(n,α)^{7}Li reaction or the ^{3}He(n,p)^{3}H reaction can be identified, depending on the gas used in the counter. Neutron detectors are also fabricated by coating the walls with a neutron reactive material (usually ^{10}B or $^{10}BC_4$) with the chamber backfilled with a common proportional-counter gas.

2.4 Geiger-Müller Counters

Although Hans Geiger originally created the gas-filled detector in 1908 (with Ernest Rutherford), the device used today is based on an improved version that Geiger's first PhD student, Walther Müller, constructed in 1928 (Geiger and Müller, 1928). Hence, the proper name for the device is the "Geiger-Müller" counter. The original "Geiger" counter was sensitive to alpha particles, but not so much to other forms of ionizing radiation. Müller's improvements included the implementation of vacuum tube technology, which allowed the device to be formed into a compact and portable tube sensitive to alpha, beta, and gamma radiation. In

1947, Sidney Liebson further improved the device by substituting a halogen as the quenching gas (Liebson and Friedman, 1948). This change in the quenching gas enabled the detector to operate at lower applied voltages over a longer lifespan. Geiger-Müller (GM) counters are typically arranged in a coaxial configuration, in which a thin anode wire is projected inside a tube that serves as the cathode. A high voltage is applied to the central anode wire, while the cathode is held at ground.

A GM counter is operated in Region IV of the gas curve and depends upon gas multiplication as a signal amplification mechanism, much like a proportional counter does. However a single important difference is that, at any specific applied voltage, all output pulses from a GM counter are of the same amplitude regardless of the ionizing radiation energy or type. This constant amplitude results from how the pulses are formed. In a proportional counter the charge cloud formation ends when the free electrons are collected. But in a GM counter the charge cloud formation ends when the space-charge buildup reduces the electric field below E_A. Because of the constant pulse amplitudes, GM counters do not intrinsically possess the ability to discriminate among alpha, beta, or gamma radiations, nor can they distinguish the different energies of these radiations.

Pulse formation time is relatively long for a GM counter, and consequently, the dead time is typically 10 times longer than that of proportional counters of similar size and is typically about 100 μs. Because GM counters are usually sealed tubes, the quenching gas inside can be exhausted over time if traditional organic molecules such as the methane component of P-10 gas are used. Instead, Geiger-Müller counters use halogens for a quenching gas, in which the diatomic molecules dissociate when they strike the cathode. Halogens, unlike methane, can heal themselves by recombining into diatomic molecules, thereby extending the life of the gas in the detector.

3 Scintillation Detectors

Scintillation detectors convert absorbed radiation energy into detectable light photons, usually in the visible light range. These light emissions can then be detected with light-sensitive instrumentation. Scintillators are generally separated into two classes: inorganic and organic scintillators. This distinction is made because the mechanisms of light production are different for scintillators in each category.

3.1 Inorganic Scintillators

Inorganic scintillators can be found as crystalline, polycrystalline, or microcrystalline materials and depend primarily on the energy band structure of the material for the production of scintillation light (McGregor, 2018). Depicted in Fig. 4 are the energy bands of inorganic scintillators. If a radiation particle interacts in the scintillator, it can excite, through a cascade of processes, numerous electrons from the valence and lower-bound bands up into the conduction bands (see Fig. 4A) or the exciton band. An exciton is an electron and hole bound together as a neutral quasi-particle. These electrons rapidly lose energy and fall back to the conduction band edge E_C. As electrons and excitons deexcite and drop back into the valence band, they can lose energy through light emissions. However, if the emitted photons have an energy equivalent to E_g, the emitted photons can be reabsorbed by the scintillator. In effect, the scintillator is opaque to its own emissions.

To eliminate this opaqueness, an impurity is added to the crystal that introduces energy states in the band gap (depicted in Fig. 4B) producing an *activated* scintillator (Birks, 1964). In an activated scintillator, the excitation process is the same as in a crystal without the activator but now a significant fraction of excited electrons can fall into the activator excited state. Subsequent transitions to the ground state release photons with sub-band-gap energies and, thus, avoid reabsorption. However, there are exceptions in which intrinsic scintillators (scintillators without a activation impurity) still work well such as bismuth germanate ($Bi_4Ge_3O_{12}$ or BGO) and barium fluoride (BaF_2) (Rodnyi, 1997).

The light emission spectrum is dependent on the activator choice and is usually spread over a continuum of energies (Lecoq et al., 2006). The configuration coordinate diagram of Fig. 5 can be used to explain the emission spectrum (Ridley, 1982; Yen et al., 2007). An electron can be excited to point B by excitation from point A, can be captured from the conduction band, or can experience exciton capture. The transition causes thermal motion and vibrational states to appear that are represented as horizontal lines in Fig. 5. Both the spatial occupancy and the electron wave function change with this transition to the excited state, and the spatial position of lowest energy changes from A to Q_{e0} (Ridley, 1982). The electron rapidly loses energy and moves to location C and can drop to location E, releasing a photon. The electron thermally loses energy and returns to location A. This change in the most probable absorption wavelength to the most probable emission wavelength is called the Stokes Shift.

Scintillator activator impurities are identified by separating them by a colon or by parentheses. For example, Tl is the activator in NaI:Tl or NaI(Tl). The intensity of light emitted at time t after radiation is absorbed in the scintillator is $I(t) = I(0)\exp(-t/\tau)$, where τ is the mean *decay time*. The brightness or light yield of a scintillator is a measure of photon yield per unit energy, with higher light yields usually producing better energy resolution.

Discovered in 1948 by Robert Hofstadter, NaI:Tl is one of the most widely used scintillators for gamma-ray spectroscopy (Hofstadter, 1949). NaI:Tl detectors do not require cooling during operation and can be used in a great variety of applications. The bare NaI:Tl crystal is hygroscopic and fragile; however, when properly packaged, they can have a long life, operate in warm and humid environments, resist a reasonable

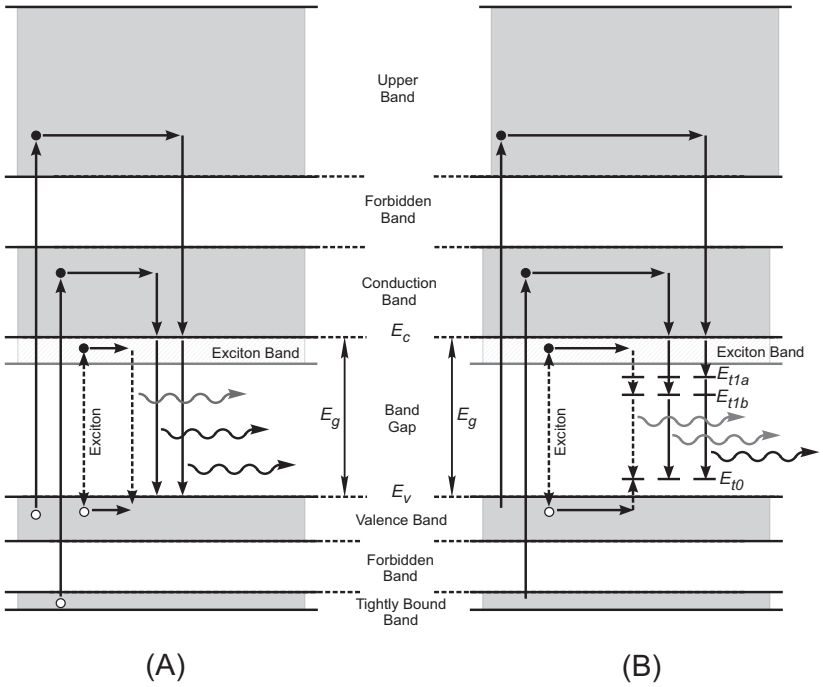

Figure 4. Shown are two basic methods by which an inorganic scintillator produces light. The intrinsic case (A) has no added activator impurities. The extrinsic case (B) has activator impurities that produce energy levels in the band gap. Copyright (2020). From Radiation Detection: Concepts, Methods and Devices by D.S. McGregor and J.K. Shultis. Reproduced by permission of Taylor and Francis Group, LLC, a division of Informa PLC.

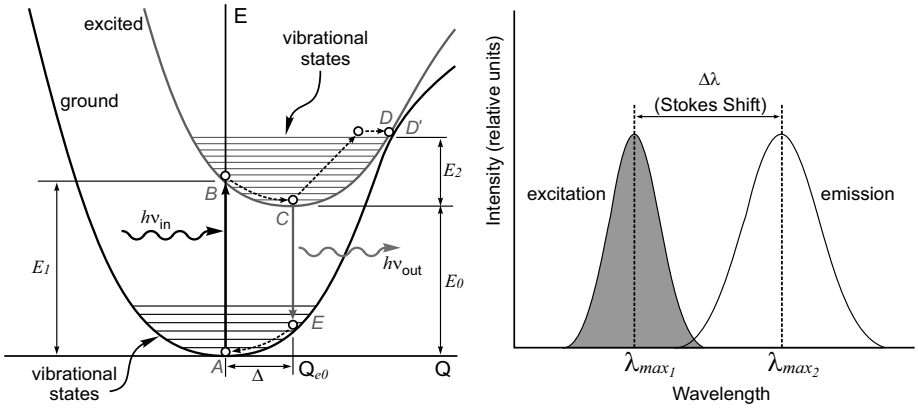

Figure 5. Configuration coordinate diagram for a luminescent center depicting luminescence with a Stokes shift and also a form of non-radiative deexcitation. The ordinate is energy E and the abscissa is the average distance Q between the luminescent center and the surrounding ions. Copyright (2020). From Radiation Detection: Concepts, Methods and Devices by D.S. McGregor and J.K. Shultis. Reproduced by permission of Taylor and Francis Group, LLC, a division of Informa PLC.

level of mechanical shock, and are resistant to radiation damage. For common applications requiring high gamma-ray efficiency and a modest energy resolution, NaI:Tl is a good choice (Shafroth, 1967).

Since the discovery of NaI:Tl, the search has continued for a scintillator with better performance for gamma-ray detection and spectroscopy. A detailed discussion of the search for new scintillators is provided by Lecoq et al. [2006] (see also McGregor and Shultis, 2020, and references therein). In recent years, $LaBr_3$:Ce, a relatively new scintillator with exceptional properties for gamma-ray spectroscopy, has become available. $LaBr_3$:Ce has a much higher light yield and a much shorter decay time than those of NaI:Tl. $Cs_2LiLaBr_6$:Ce (CLLB:Ce) and Cs_2LiYCl_6:Ce (CLYC:Ce) both have good gamma-ray spectroscopic performance with the added benefit of being neutron sensitive from the ^{6}Li(n,t)^{4}He reaction. $Bi_4Ge_3O_{12}$ (BGO) has a much better detection efficiency than NaI:Tl, but somewhat inferior energy resolution. A comparison of spectroscopic performance between three commercially available scintillators is shown in Fig. 6.

3.2 Organic Scintillators

Organic scintillators depend primarily on the molecular structure of the material for the scintillation mechanism (Birks, 1964). A typical Jablonski energy diagram is shown in Fig. 7 for an organic scintillator. An independent molecule of organic scintillation material can have an electron excited through the π states up from the ground state into an excited singlet state, of which there are many levels. There are many vibrational levels associated with the ground states, typically denoted by S_{0x} where x refers to one of the vibrational sub-states. There are also numerous excited singlet states as well as excited triplet states associated with the carbon π bonds. Electrons that gain energy rise to one of the excited vibrational states and generally fall rapidly to the lowest S_{10} state, which then deexcite through two possible channels. If the electrons deexcite directly from the S_{10} state to one of the S_{0x} states, the light emission is rapid and is referred to as scintillation fluorescence. Decay times for fluorescence are typically only a few nanoseconds, and fluorescent emission can be easily linked to individual radiation events. However, if the electrons deexcite by crossing to the triplet states T_{1x} and then eventually fall to one of the S_{0x} states, the light emission is slow and is referred to as scintillation phosphorescence (Birks, 1964). This second light producing mechanism is undesirable because phosphorescent emission is slow and continues to produce afterglow for extended periods of time and, hence, can not be directly linked to individual radiation events, especially in high-radiation

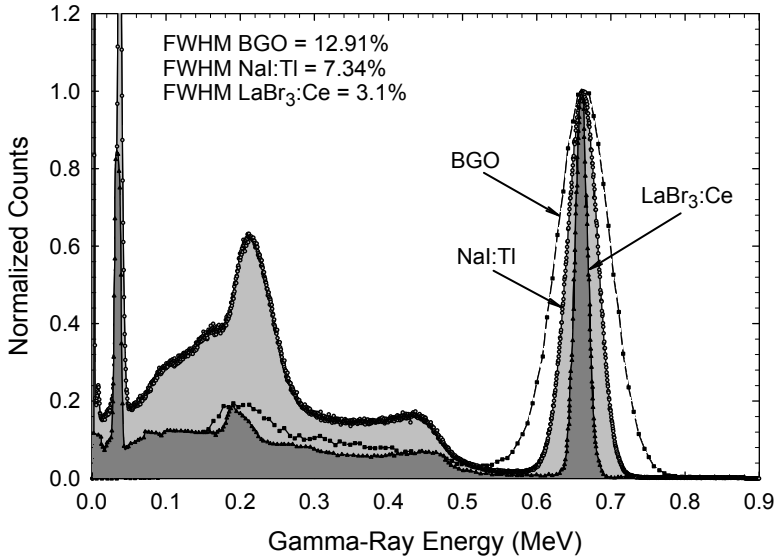

Figure 6. Comparison of normalized spectral performance for a 2×2 NaI:Tl detector, a 2×2 $LaBr_3$:Ce detector, and a BGO detector of similar size for 662-keV gamma rays from ^{137}Cs. Copyright (2020). From Radiation Detection: Concepts, Methods and Devices by D.S. McGregor and J.K. Shultis. Reproduced by permission of Taylor and Francis Group, LLC, a division of Informa PLC.

fields.

Organic scintillators are composed mostly of hydrogen and carbon, both of which are poor absorbers of gamma rays. Organic scintillators have nonlinear light output for heavy ion radiation, yet much more linear in response to electrons and beta particles. Organic scintillators are frequently used for beta particle and electron detection (NCRP, 1985). Because much of the energy of fast neutrons, upon scattering from H, is transferred to the recoil proton, organic scintillators are often used for fast neutron detection by detecting the recoil protons.

Organic scintillators depend on the molecular structure, often a benzene ring structure, and do not need activator dopants for the scintillation mechanism. Hence, they also need not be crystalline or polycrystalline in structure. As a result, organic scintillators can be formed as solids, liquids, gases, and plastics. Liquid scintillators are commonly used for beta particle measurements, where the radioactive material is mixed in a "cocktail" solution of fluor and solvent (Horrocks and Peng, 1971; NCRP 1985). Small amounts of materials can be mixed in the organic scintillator without destroying the scintillation process. For instance ^{10}B, ^{6}LiF, or Gd can be mixed into the scintillator to enhance thermal neutron sensitivity while heavy metal particles, such as Pb, can be added to increase gamma-ray sensitivity.

3.3 Light Collection

Although a scintillator produces a light signal when a radiation particle interacts in the scintillator, the light must be converted to an electronic signal if it is to be recorded. Below, four devices for doing such a conversion are discussed.

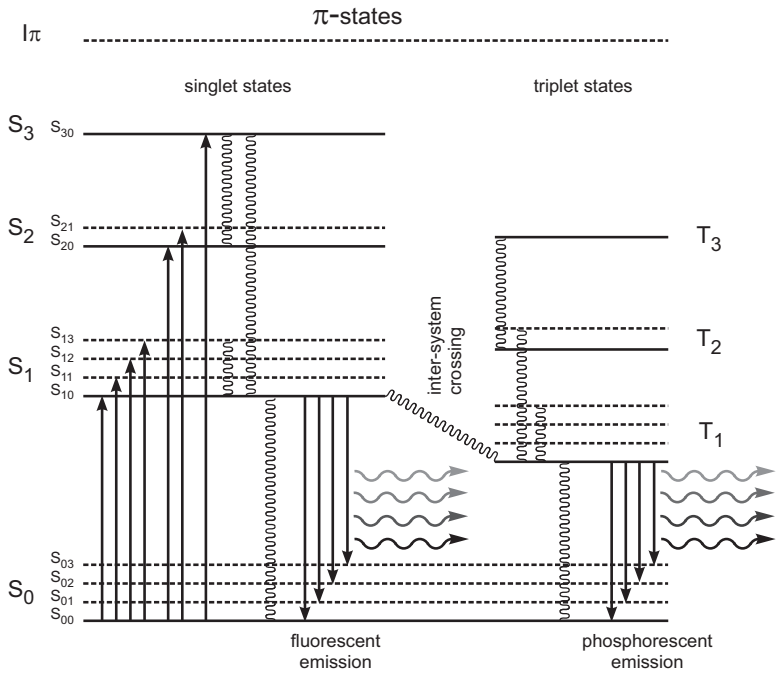

Figure 7. Shown are two basic methods by which an organic scintillator produces light. After Birks [1964].

3.3.1 Photomultiplier Tubes

Secondary electron emission was discovered in 1902 by Austin and Starke when they noticed that exposing metal surfaces to cathode rays (electrons) caused the emission of more electrons than were incident. In 1919, Slepian proposed, and patented, the concept of using secondary electron emission as an amplification device (Slepian, 1923). Some attempts were made to use the process with vacuum tube technology, but it was not until 1941 that the RCA Company released the first amplifier tube, called a photomultiplier tube (PMT), that used secondary electron emission for signal amplification (Engstrom, 1980). This PMT, the RCA Type 931, was originally used as a signal amplifier for electronics, and was used for radar jamming technology during the Second World War.

In 1947 Broser and Kallman (1947a; 1947b) coupled a PMT to the organic scintillator naphthalene and produced the first scintillation detector system. In 1948 Hofstadter discovered the inorganic scintillator NaI:Tl, which when coupled with a PMT produced the first practical solid-state gamma-ray spectrometer.

The basic PMT, depicted in Fig. 8, has a photocathode to absorb light emissions from a light source such as a scintillating material (see Engstrom, 1980). Light photons that strike the photocathode excite electrons that can then diffuse to the surface facing the vacuum side. A fraction of these electrons escape the surface into the vacuum tube. A voltage applied to the tube accelerates and guides these electrons to the first *dynode* electrode. When an electron strikes the dynode, it again causes more electrons to become liberated into the tube. These newly liberated electrons are then guided to the next dynode where more electrons are liberated and so on. As a result, the total number of electrons eventually released depends on the number of dynodes in the PMT and the photoefficiency of the photocathode and the dynodes.

The total charge released in the PMT is $Q = qN_0G^n$, where q is the charge of an electron, N_0 is the initial number of electrons released at the photocathode and that reach the first dynode, G is the number of electrons released per dynode per incident electron (the gain), and n is the total number of dynodes in

the PMT. For instance suppose that a PMT has 10 dynodes each operated with a gain of 4. An event that initially releases 1000 electrons (N_0) causes over 10^9 electrons to emerge from the PMT.

PMTs are stable and electronically quiet (low noise). Modern varieties have high photocathode and dynode efficiencies, often referred to as *quantum efficiency*, with gains that can exceed 30. Photocathodes are generally made from alkaline metals, which are most sensitive to light in the 350 to 450 nm range (Donati, 2000). Scintillators emitting light outside this range can still be used under some circumstances, although their effectiveness can be compromised.

3.3.2 Microchannel Plates

Microchannel plates are an alternative method for amplifying signals from a scintillator. Microchannel plates are glass tubes whose insides are coated with secondary-electron emissive materials. A voltage is applied across the tube length which causes electrons to cascade down the tube. Every time an electron strikes the tube wall, more electrons are emitted, much like with dynodes in a PMT. Hence, a single electron entering the tube can cause a cascade that can eventually produce 10^6 electrons emitted from the other end of the tube (Donati, 2000). Typically, hundreds of these microchannels are bonded together to form a plate of channels running in parallel. The microchannel plate can be fastened to a scintillator to operate in a similar fashion as a PMT. Light photons entering the microchannel plate cause the ejection of primary photoelectrons, which cascade down the microchannels to liberate millions more electrons. The main advantage of a microchannel plate over a PMT is its compact size. A microchannel plate only one inch thick can produce a signal of similar strength as a PMT. The main problem with microchannel plates is the signal produced per monoenergetic radiation event is statistically much noisier than that produced by a PMT, hence the energy resolution for spectroscopy is typically worse than that provided by a PMT.

3.3.3 Photodiodes

Photodiodes are semiconductor devices formed into a *pn* or *pin* junction diode (Sze, 1981). When photons strike the semiconductor, usually Si or GaAs based materials, electrons are excited. A voltage bias across the diode causes the electrons to drift across the device and induce charge much as occurs in a gas-filled ion chamber. The quantum efficiency of the semiconductor diode varies with the configuration and packaging

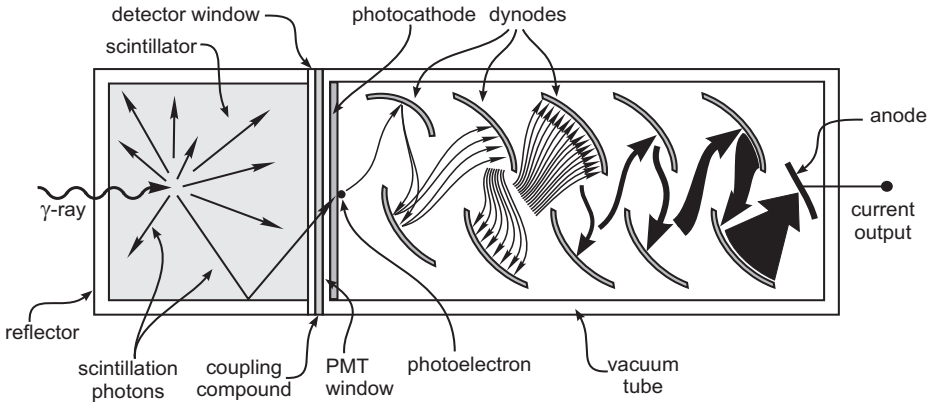

Figure 8. The basic mechanisms of a photomultiplier tube (PMT). An absorbed γ ray causes the emission of numerous light photons, some of which reach the photocathode. Electrons emitted from the photocathode are then amplified in number by a chain of dynodes. Copyright (2017). From Nuclear Science and Engineering by J.K. Shultis and R.E. Faw. Reproduced by permission of Taylor and Francis Group, LLC, a division of Informa PLC.

of the diode. For instance, various different commercial Si photodiodes have peak efficiencies at wavelengths ranging between 700 to 1000 nm (Sze, 1981; Donati, 2000). Regardless, they are typically more sensitive to longer wavelengths than commercial PMTs. As a result, emissions from CsI:Tl, a relatively bright scintillator with most probable emissions near 550 nm, match better to Si photodiodes than PMTs. Photodiodes operate with low voltage, are small, rugged, and relatively inexpensive. Thus, they provide a practical and compact method of sensing light emissions from scintillators. However, they typically do not couple well to light emissions near the 400 nm range (blue-green) and have low gain, if any at all. Consequently, the signals from photodiodes need more amplification than signals from PMTs, and scintillator/photodiode systems generally do not have an energy resolution as good as that of scintillator/PMT systems.

3.3.4 Silicon Photomultipliers

A single photon avalanche diode (SPAD) can be used to increase the signal gain (Cova et al., 1989). The device is designed such that an electric field in the diode is sufficiently high to cause impact ionization of more electrons, in a similar fashion as occurs in proportional and Geiger-Müller counters. If the device is overly biased, beyond stability, then a single photon can trigger an avalanche (Haitz, 1961; McIntyre, 1961). The avalanche can be quenched by including a resistor in series with the diode. As the current increases, the voltage across the resistor also increases, thereby reducing the SPAD voltage below the critical electric field strength and, thereby quenching the avalanche.

An array of SPADs can be fashioned into a type of silicon photomultiplier (SiPM) (Renker, 2006). The device operates under the assumption that, statistically, a single SPAD will intercept no more than one photon per scintillation shower. Each SPAD is designed and biased such that they all produce approximately the same signal output, much like the GM counter. Consequently, the total output voltage can be divided by the average voltage per SPAD to determine the total number of photons in the shower. Nonlinearities can arise from high-energy gamma rays interacting in exceptionally bright scintillators such that more than one photon strikes an SPAD simultaneously. The consequence is that the SPAD cannot distinguish between one or more photons, and the SiPM output voltage will underestimate the true number of photons and the associated gamma-ray energy.

SiPMs are compact and rugged devices, and are generally unaffected by magnetic fields. In recent years, SiPM technology has become a popular alternative to PMTs for commercial scintillation detectors.

4 Semiconductor Detectors

Perhaps the first reported attempt of producing a solid-state conduction counter is by Röntgen and Joffé [1913] on various solids, yielding mostly unsuccessful to marginal results. The first successful semiconductor detectors were reported by Stetter in 1941 (with diamond samples) and then by Van Heerden in 1945 (AgCl samples). Although afterwards various other semiconductors were developed and tested for novel radiation detection applications, it was not until Pell introduced the Li drifting compensation method in 1960 did certain semiconductors (mainly Si and Ge) become important radiation detectors.

The operation of a semiconductor detector combines the the charge excitation process in a crystalline inorganic scintillator and the charge collection method of a gas-filled ion chamber. Shown in Fig. 9, gamma rays or charged particles absorbed in the semiconductor excite electrons from the valence and tightly bound energy bands up into the numerous (and almost continuum of) conduction bands. The empty states left behind by the negative electrons act as positively charged particles, called *holes*. The excited electrons rapidly deexcite to the conduction band edge E_C. Likewise, as electrons high in the valence band fall to lower empty states in the valence and tightly bound bands, the holes appear to move upwards towards the valence band edge E_V.

The principal difference between a semiconductor and almost all scintillators is that the mobility of charge carriers in semiconductors is sufficiently high to allow conduction, whereas scintillation materials are mostly

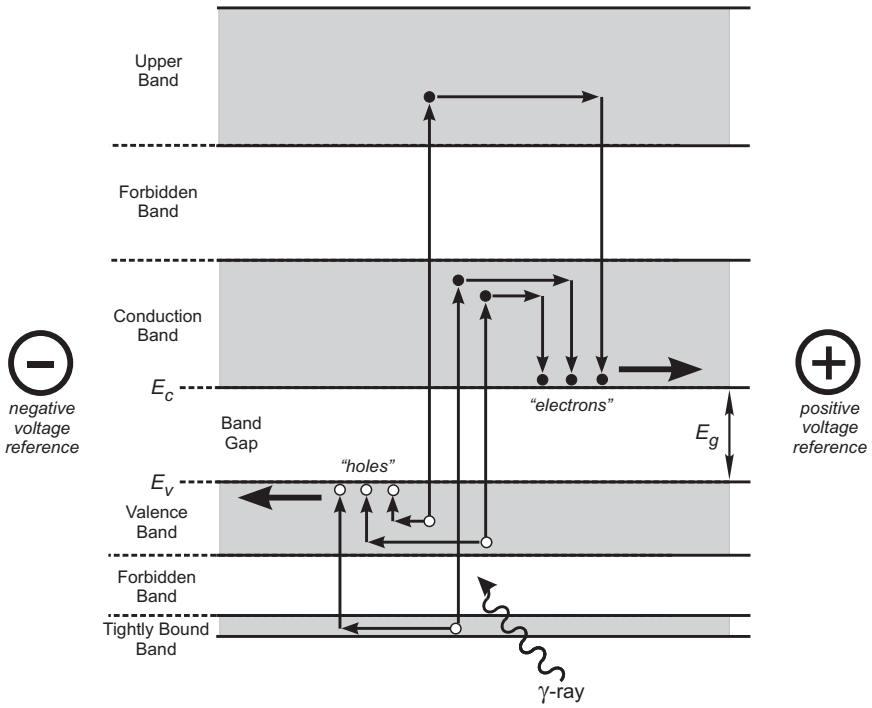

Figure 9. Absorbed radiation energy excites electrons from the valence and tightly bound bands up into the higher conduction bands. The empty states (*holes*) left behind mimic positive charge carriers. The electrons quickly deexcite to the lowest conduction band edge E_C and the holes rapidly deexcite to the top of the valence band E_V. A voltage applied to the detector causes the electron and hole charge carriers to drift to the electrodes. Copyright (2017). From Nuclear Science and Engineering by J.K. Shultis and R.E. Faw. Reproduced by permission of Taylor and Francis Group, LLC, a division of Informa PLC.

insulating materials that do not conduct. As a result, a voltage can be applied across a semiconductor material to cause the negative electrons and positive holes, commonly referred to as *electron-hole pairs*, to drift in opposite directions, much like the electron-ion pairs do in a gas-filled ion chamber. In fact, at one time semiconductor detectors were referred to as "solid-state ion chambers" (Price, 1964). As these charges drift across the semiconductor, they induce a current to flow in an external circuit which can either be measured as a current or stored across a capacitor to form a voltage.

Semiconductors are far more desirable for energy spectroscopy than gas-filled detectors or scintillation detectors because they are capable of much higher energy resolution. This observed resolution improvement is largely due to the better statistics resulting from the more numerous charge carriers produced by a radiation interaction (Bertolini and Coche, 1968). Typically, it only takes between 3 to 5 eV to produce an electron-hole pair in a semiconductor (McGregor and Hermon, 1997; Owens, 2019), whereas 25 to 35 eV are required to produce an ion-electron pair in most gases (Sauli, 2014). Some common semiconductors and their properties are listed in Table 1.

Most semiconductor detectors are configured as either planar or coaxial devices, as depicted in Fig. 10. Small semiconductor detectors are configured as planar devices and can be used for charged-particle detection and gamma-ray detection (Dearnaley and Northrop, 1966). Large semiconductor gamma-ray spectrometers

Table 1. Common semiconductors and their properties.

Semiconductor	At. Number (Z)	Density (g cm^{-3})	Band Gap (eV)	Ionization Energy (eV/e-h pair)
Si	14	2.33	1.12	3.61
Ge	32	5.33	0.72	2.98
GaAs	31/33	5.32	1.42	4.2
CdTe	48/52	6.06	1.52	4.43
$Cd_{0.9}Zn_{0.1}Te$	48/30/52	6.0	1.60	5.0
HgI_2	80/53	6.4	2.13	4.3

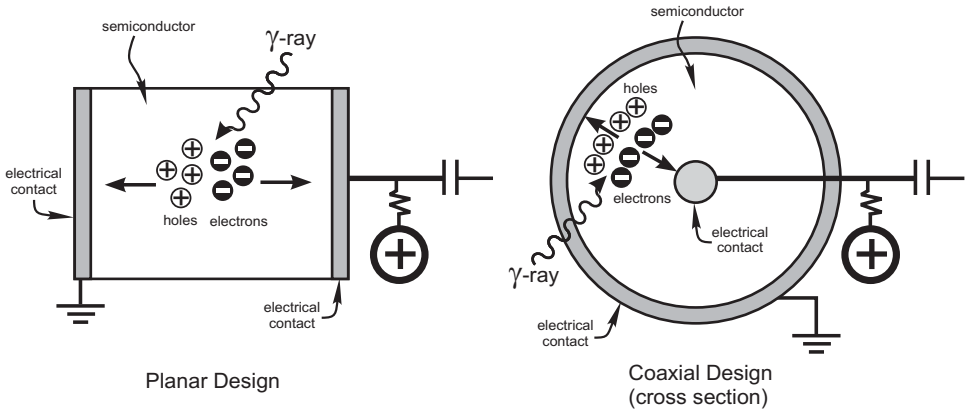

Figure 10. The two most common designs for semiconductor detectors are the planar and coaxial configurations. Copyright (2017). From Nuclear Science and Engineering by J.K. Shultis and R.E. Faw. Reproduced by permission of Taylor and Francis Group, LLC, a division of Informa PLC.

are usually configured in a coaxial geometry to reduce the detector capacitance. Refrigeration with cryogenics or mechanical coolers are used with many large semiconductors, usually Ge and Si devices, to reduce thermally generated leakage currents. To reduce injected leakage current, semiconductors are formed as reverse biased diodes, which can be Schottky, *pn*, or *pin* junction devices. Under some special conditions, highly resistive semiconductors need only have ohmic contacts because the bulk resistance is adequate to reduce leakage currents (McGregor and Shultis, 2020).

4.1 Ge Detectors

In 1960, Pell introduced the technique for drifting Li ions into a silicon semiconductor to counteract the deleterious effects of impurities (Pell, 1960). Within a fews years, the same technique was adopted for Ge detectors (Brown et al., 1969). Unfortunately, if a lithium-drifted Ge [or Ge(Li)] detector warms to room temperature, the Li diffuses from compensation sites and the detector is ruined (Bertolini and Coche, 1968). Consequently, Ge(Li) detectors must always be keep at liquid nitrogen (LN2) temperatures. Modern Ge detectors are made from high-purity zone-refined material and no longer require Li compensation. However, a high purity Ge (HPGe) detector must still be chilled with LN2 or a refrigerator *when operated* in order to reduce thermally generated leakage currents.

HPGe detectors have exceptional energy resolution compared to scintillation and gas-filled detectors. Comparison spectra between a NaI:Tl and a HPGe spectrometer are shown in Fig. 11. HPGe detectors

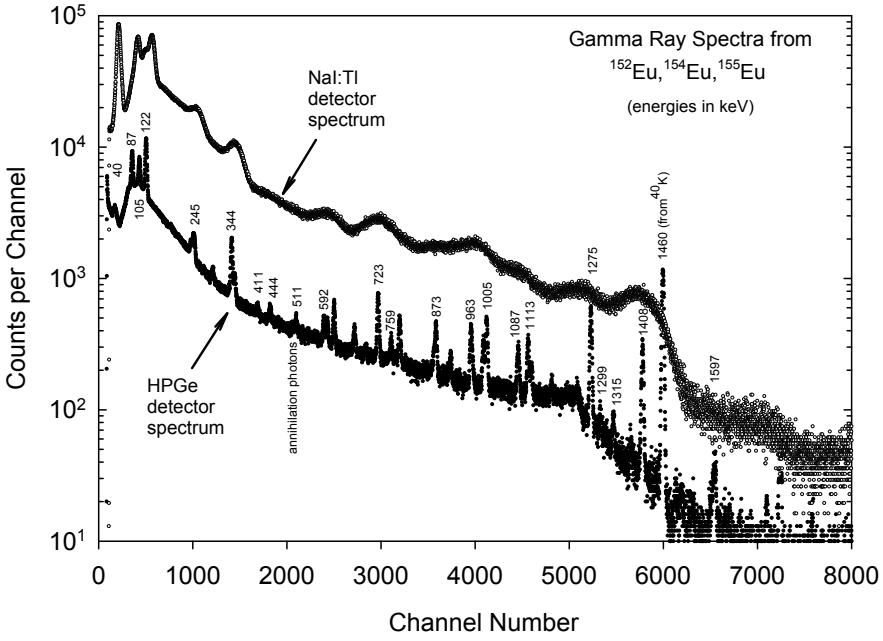

Figure 11. Comparison of the energy resolutions of a NaI:Tl and an HPGe detector. The gamma-ray source is a mixture of the radioisotopes ^{152}Eu, ^{154}Eu, and ^{155}Eu. Copyright (2017). From Nuclear Science and Engineering by J.K. Shultis and R.E. Faw. Reproduced by permission of Taylor and Francis Group, LLC, a division of Informa PLC.

are now standard high-resolution spectroscopy devices used in the laboratory. Their high energy resolution allows them to easily identify radioactive isotopes for a variety of applications such as impurity analysis, composition analysis, and medical isotope characterization, to name a few. Portable devices with small LN2 dewars or compact efficient refrigerators are also available for remote spectroscopy measurements.

Because of the higher atomic number of iodine and the generally larger size of NaI crystals, NaI:Tl detectors often have a higher detection efficiency for gamma rays than do HPGe detectors. Historically, the efficiency of a Ge detector was commonly compared to that of 3-inch diameter × 3-inch long (3×3) right circular cylinder of NaI:Tl for ^{60}Co gamma-ray energies (Tsoulfanidis and Landsberger, 2015). This standard continues today, where the efficiency of an HPGe detector is quoted in terms of a 3×3 NaI:Tl detector. For example, a 60% efficient HPGe detector has 60% of the efficiency that a 3×3 NaI:Tl detector has for ^{60}Co gamma rays. HPGe detectors are much more expensive than NaI:Tl detectors; hence, they are best used when gamma-ray energy resolution is of importance whereas NaI:Tl detectors provide higher efficiency for measuring somewhat weak gamma-ray radiation fields.

4.2 Si Detectors

The problem with Li redistribution in Ge(Li) crystals when the detector warms does not apply to Si (Bertolini and Coche, 1968). Hence, Si(Li) detectors are still available in spite of their relatively poor efficiency for energetic photons. Because Si has a much lower average atomic number than Ge, the relative efficiency of Si(Li) to HPGe per unit thickness is significantly lower for electromagnetic radiation. However, for x-ray or gamma-ray energies less than about 30 keV, commercially available Si(Li) detectors are thick enough to provide performance comparable to HPGe detectors. For example, a 3 to 5 mm thick Si(Li) detector with

a thin entrance window has an efficiency of almost 100% for 10-keV photons. Si(Li) detectors are preferred over HPGe detectors for low energy x-ray measurements, primarily because of the lower energy x-ray escape peak features that appear in a Si(Li) detector spectrum as opposed to an HPGe detector spectrum (Goldstein et al., 1981). Further, background gamma rays, which complicate an x-ray spectrum, tend to interact more strongly in HPGe detectors than in Si(Li) detectors. Because a majority of the applications require a thin window, Si(Li) detectors are often manufactured with very thin beryllium windows (McGregor and Shultis, 2020). Typically, Si(Li) detectors are chilled with LN2 to reduce thermal leakage currents to allow optimum performance.

High-purity Si detectors without Li drifting are also available, but are significantly smaller than HPGe and Si(Li) detectors. Such devices are typically only a few hundred microns thick and are designed for charged-particle spectroscopy (McGregor and Shultis, 2020). They range in diameter from one centimeter to several centimeters. The detectors are formed as diodes to reduce leakage currents, and use either a Schottky contact or a thin implanted *pn* junction contact to produce a rectifying diode. These devices are operated in reverse bias to reduce leakage currents. To reduce energy loss through the contact dead layer, the contacts and junctions are kept thin, typically being only a few hundred nanometers. Measurements are typically conducted in a vacuum chamber to reduce particle energy loss in air. Because the detectors are thin, they have low thermal generation of charge carriers and, consequently, can be operated at room-temperature.

4.3 Alternative Semiconductor Detectors

The fact that HPGe and Si(Li) detectors must be chilled during operation is a considerable inconvenience. Much research has been devoted to finding semiconductors that can be used at room temperature (Owens, 2012). The main requirement is that the band-gap energy be greater than 1.4 eV to reduce thermally generated leakage currents (McGregor and Hermon, 1997). For gamma-ray detection, the material is best composed of high atomic number elements. Consequently, there are only a few possibilities, all of which are compound semiconductors, meaning that they are composed of two or more elements. Three important semiconductors used for room-temperature operation are HgI_2, CdTe, and CdZnTe.

Mercuric iodide (HgI_2) has been studied since the early 1970s as a candidate gamma-ray spectrometer material and has been used for commercial x-ray spectrometry analysis (Willig, 1971; Malm, 1972). The high atomic numbers of Hg ($Z = 80$) and iodine ($Z = 53$) make it attractive as an efficient gamma-ray absorber, and its large band gap of 2.13 eV allows it to be used as a room temperature gamma-ray spectrometer.

Cadmium telluride (CdTe) has been studied since the mid-1960s as a candidate gamma-ray spectrometer material (Autagawa et al., 1967; Mayer, 1967). It has relatively good gamma-ray absorption efficiency with Cd ($Z = 48$) and Te ($Z = 52$). The band gap of 1.52 eV also allows CdTe to be operated at room temperature. There are commercial vendors of CdTe detectors but the devices are relatively small, typically a few mm thick with an area of a few mm^2. CdTe detectors have been used for room-temperature-operated low-energy gamma-ray spectroscopy systems, and also for electronic personnel dosimeters.

Cadmium zinc telluride (CdZnTe or CZT) has been studied as a gamma-ray spectrometer since 1992 (Butler et al., 1992; Doty et al., 1992). One of the most studied versions of CZT has 10% Zn, 40% Cd, and 50% Te molar concentrations, a composition which yields a material with a band-gap energy of approximately 1.6 eV. CZT detectors offer an excellent option for low-energy x-ray spectroscopy when cooling is not possible. Although the detectors are quite small compared to HPGe and Si(Li) detectors, they are manufactured in sizes ranging from 0.1 cm^3 to 2.5 cm^3. Because of their small size they perform best at gamma-ray energies below 1.0 MeV. Various clever electrode designs have been incorporated into new CZT detectors to improve their energy resolution, and CZT has become the most used compound semiconductor for gamma-ray spectroscopy (Owens, 2012; McGregor and Shultis, 2020).

5 Personnel Dosimeters

An important application of radiation detection is to measure the radiation dose received by workers in a radiation environment. Here the most common personnel dosimeters are discussed. These dosimeters can, or course, also be used as area monitors to measure the accumulated exposures at various locations in a radiation environment.

5.1 Photographic Film

Photographic film is one of the oldest radiation detection devices, having been used by Röntgen after his discovery of x rays in 1895. The *film badge* consists of a packet of photographic film sealed in a holder with various attenuating filters (McGregor and Shultis, 2020). Ionizing radiation darkens the film as in the production of an x-ray image. The filtration is designed to modify the degree of film darkening, as nearly as possible, to a known function of gamma-ray exposure, independent of the energy of the incident gamma rays. After the badge is carried by a radiation worker for a period of time, the film is processed, along with calibration films with the same emulsion batch exposed to known radiation doses. The worker's radiation dose for the period is assessed and ordinarily maintained in a lifetime record of exposure. In some cases, special attenuation filters are used to relate the darkened portions of the film to beta-particle or even neutron dose. Special badge holders in the form of rings or bracelets are used to monitor the radiation exposure of hands, wrists, and ankles (Cember, 1983).

5.2 Pocket Ion Chambers

A compact form of ion chamber closely related to an electrometer is the *pocket ion chamber*. These devices are routinely used to measure the radiation dose received by the wearer (Cember, 1983). The device consists of a tube approximately 10 cm long and 1 cm in diameter. Inside the tube are two small metal-coated quartz fibers, each approximately 4 microns in diameter. One of the quartz fibers is stationary and the other is hinged, and both are inside an air cavity of the tube. The tube also has viewing optics such that when held up to a light, the observer can see the shadow of the hinged quartz fiber against a dose scale. The chamber is inserted into a power supply and charged so the two fibers, having like charges, are spread apart. This charged device can now be worn as a dosimeter. Electrons excited by radiation interactions in the air cavity are attracted to the quartz fibers and reduce the charge on the quartz fibers causing these fibers to move closer together (Eichholz and Poston, 1979). The change in location of the hinged fiber with respect to the metered display yields the dose (the scale maximum is usually 200 mR) (Cember, 1983).

5.3 TLDs and OSLs

Thermoluminescent dosimeters (TLDs) and optically stimulated luminescent (OSL) dosimeters are used for radiation dosimetry measurements. Both TLD and OSL dosimeters are reusable and can be worn as personnel dosimeters. They can be read out for dose, cleared, and used again repeatedly. Select areas of an OSL dosimeter can be read out, with the unread areas still available for sampling at a later date. However, once a TLD dosimeter is read, the dose information is cleared and can not be reevaluated. Dosimeters are checked periodically, between a few weeks to a month, and hence do not yield immediate information about radiation exposure. Rather, they are used to record the radiation dose accumulated by the wearer.

TLDs and OSLs consist of small polycrystals held together by a binder. These polycrystals behave similar to a common scintillator with some important differences. Electrons elevated in energy from ionizing radiation can either recombine with holes or they can drop into *traps*. These traps are engineered into the bandgap by the introduction of specific impurities, and they can retain electrons for long periods of time.

When a TLD is heated, the trapped electrons are released and can fall through luminescent centers to release light (McKeever, 1985). TLDs are gradually heated up to a maximum temperature ($\leq 400°C$) that

ensures the complete release of all trapped electrons (Cameron et al., 1968). The light output is measured with a PMT as a function of the TLD temperature. The resulting displayed output (light vs temperature) is referred to as a *glow curve* (Cameron et al., 1968). Glow curves are unique to the TLD material type and impurity. The total light output varies linearly with the absorbed dose. If a TLD is not read out within a reasonable amount of time after the radiation exposure ($\sim$ 1 or 2 months), a substantial number of electrons can return to the ground state. This effect is referred to as *fading* and causes some information about the radiation dose to be lost (Cameron et al., 1968).

Although there are many useful TLD materials, the most common are lithium fluoride (LiF), calcium fluoride (CaF_2), and calcium sulphate ($CaSO_4$) (McGregor and Shultis, 2020). LiF fluoride has a density similar to human tissue and is more popular than other TLD materials for personnel dosimetry. Neutron sensitive LiF TLDs are fabricated with enriched ^{6}Li labeled TLD-600. Upon absorbing a neutron, energetic reaction products are released that are recorded by the TLD. Neutron insensitive TLDs can be made from LiF enriched with ^{7}Li labeled TLD-700. Paired together, they can provide information on the gamma-ray and neutron doses.

OSL dosimeters have become popular over the last few decades and have in many cases replaced TLDs (Bøtter-Jensen et al., 2003; Yukihara and McKeever, 2011). OSL dosimeters are usually carbon activated samples of Al_2O_3, and behave almost exactly the same as TLDs. Electrons are excited into the impurity traps where they stay lodged until the OSL dosimeter is read. However, instead of thermal excitation, trapped electrons in OSL dosimeters are dislodged with laser stimulation which can be directed to specific locations on the sample. The total light released by the OSL dosimeter is linearly related to the total accumulated dose. OSL dosimeters are more sensitive than TLDs to low levels of radiation and are capable of recording doses below 1 mrad.

6 Alternative Detectors

There are many novel radiation detectors, some unique, that are built to reveal the paths of radiation particles, to detect radiation through new physical mechanisms, or to record exotic radiations such as neutrinos and mesons. The description of the many specialized detectors, particularly those used in high-energy physics research, would require a separate chapter. Here just a few of these unusual detectors are introduced. Detailed discussions can be found in the literature and associated references (McGregor and Shultis, 2020).

6.1 Cloud Chambers, Bubble Chambers, and Superheated Drop Detectors

Charles Wilson invented the cloud chamber in 1911, a device used to detect ionizing charged particles (Wilson, 1911; 1912). A cloud chamber is a sealed transparent container holding a supercooled, supersaturated vapor of water, alcohol, or aromatic hydrocarbon. Alpha particles or beta particles ionize the saturated vapor as they pass through it. The ionized vapor molecules form nucleation centers for condensation and a visible mist forms along the ionization track. Wilson shared the 1927 Nobel Prize in Physics for inventing the cloud chamber.

Donald Glaser invented the bubble chamber in 1952, a type of detector closely related to the cloud chamber (Glaser, 1952). The bubble chamber is a vessel filled with a superheated transparent liquid used to detect charged particles as they move through the liquid. Charged particles deposit sufficient energy in the liquid so that it begins to boil along the ionization track, thereby forming a visible string of bubbles. Glaser received the 1960 Nobel Prize in Physics for inventing the bubble chamber.

In 1979, Robert Apfel invented the superheated drop detector, which is similar to the cloud chamber and the bubble chamber (Apfel, 1979). A fluid can be superheated to temperatures and pressures corresponding to the vapor region in the phase diagram. This metastable state is fragile and typically short-lived due to the high number of microscopic particles or gas pockets normally present at the container surfaces.

However, a liquid may be kept in steady-state superheated conditions by fractionating it into droplets and dispersing them in an immiscible host fluid, for example, suspending freon droplets in a gel solution. This procedure creates perfectly smooth spherical interfaces, free of nucleating impurities or irregularities. Radiation particles, including neutrons, interacting in the fluid can disrupt this balance between the liquid and vapor phase of a superheated droplet, causing it to burst into a sizable bubble of vapor. Bubble formation is measured from the volume of vapor expelled or by detecting individual vaporizations acoustically, i.e. "listening" to the radiation interactions.

6.2 Cryogenic Detectors

Radiation detectors that are becoming increasingly more interesting are the cryogenic or low-temperature devices (Enss, 2005). One such device is the *microcalorimeter*. These cryogenic devices sense the change in temperature of an absorber material caused by a single radiation quantum event in it. The device operates by attaching a small sample of thermally conductive material to a cryogenic refrigerator platform, and the sample is cooled to milli-Kelvin temperature levels with a refrigerator (such as a liquid-helium refrigerator or portable mechanical refrigerator). When a single quantum of radiation, such as a gamma ray or neutron, interacts in the chilled material, the temperature change ΔT in the material is measured and recorded. Because the temperature change is a linear function of the energy absorbed, a spectrum is accumulated as a function of temperature change. Extremely high resolution spectroscopy is possible, nearly 20 times better than achievable with Si(Li) detectors. Because the device must rapidly disperse the heat, the detector samples must be small. Consequently, cryogenic detectors work best for low-energy gamma rays and x rays.

7 Radiation Counting

No measurement can be exact. There always are errors and uncertainties. With radiation measurements there is also the stochastic nature of radiation sources that leads to further uncertainties. In this section, such concerns are addressed.

7.1 Types of Measurement Uncertainties

The analysis of any type of experimental data always requires an assessment of the uncertainties associated with each measurement. Without such an uncertainty estimate, the data have very limited value. There are several types of uncertainties associated with any measurement. These include stochastic and sampling uncertainties and errors as well as systematic errors. For example, the decay of radioactive atoms occurs stochastically so that a measurement of the number of decays in a fixed time interval has an inherent stochastic uncertainty. Repeated measurements would give slightly different results. *Systematic* errors are introduced by some constant bias or error in the measuring system and are often very difficult to assess since they arise from biases unknown to the experimenter. *Sampling errors* arise from making measurements on a population different from the one desired. These biases too are hard to detect, let alone quantify.

Engineers and scientists must always be aware of the difference between *accuracy* and *precision*, even though popular usage often blurs or ignores the important distinction. Precision refers to the degree of measurement quantification as determined, for example, by the number of significant figures. Accuracy is a measure of how closely the measured value is to the true (and usually unknown) value. A very precise measurement may also be very inaccurate.

7.2 Uncertainty Assignment Based Upon Counting Statistics

Data measured with an ionizing-radiation detection system embody both random uncertainties and systematic errors. Uncertainty assignment requires knowledge of both. Even with a perfect measurement system capable of operating over a long time period without introducing significant systematic error, one must always

consider the random nature of the data caused by the stochastic nature of the radiation source such as the decay of radionuclides in a sample. This section deals only with one component of the total uncertainty—the random or statistical uncertainty.

The binomial distribution describes the basic statistical distribution for the stochastic process of radioactive decay. However, the binomial probability distribution function is numerically difficult to use for a large number of radionuclides. For a large number of radionuclides, the probability of observing a single distingration within a specified time interval is small ($\ll$1). Also, the total expected number of observed disintegrations within that time is large (typically > 20). Hence, the Gaussian distribution approximates well the probability of observing x disintegrations about dx in some specified time period, namely,

$$G(x)dx = \frac{1}{(\sqrt{2\pi})\sigma} \exp\left[-\frac{(x-\mu)^2}{2\sigma^2}\right] dx, \tag{1}$$

where $G(x)$ is the Gaussian or normal probability distribution function, μ is the expected value of the random variable x being observed, and σ^2 is the variance of the distribution. Note that the number of counts x is treated as a continuous variable that can even assume unrealistic negative values, whereas the observed number of counts must always be a non-negative integer. A typical Gaussian distribution is shown in Fig. 12, where it has been normalized to unit height.

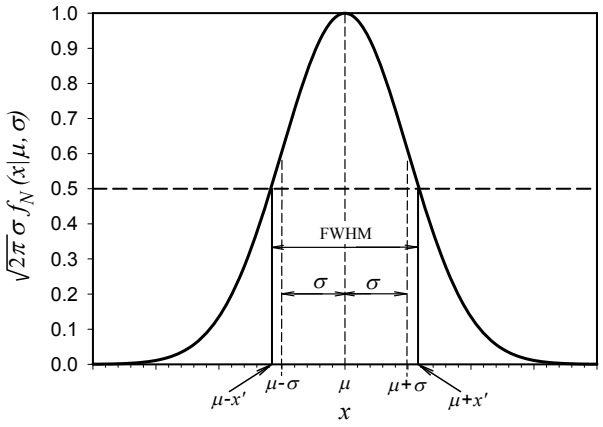

Figure 12. The Gaussian or normal distribution describes the expected probability distribution for radiation counting, where μ is the expected number of counts observed and σ is the standard deviation. From Radiation Detection: Concepts, Methods and Devices by D.S. McGregor and J.K. Shultis. Reproduced by permission of Taylor and Francis Group, LLC, a division of Informa PLC.

Data are routinely reported as $\overline{x} \pm \sigma_{\overline{x}}$ where $\overline{x}$ is the average number of measured counts during a specified time period and $\sigma_{\overline{x}}$ is the *standard deviation* of $\overline{x}$ (Bevington and Robinson, 1992). When an error is reported as one standard deviation (or "one sigma") it is called the *standard error*. For a single measurement x of a radioactive sample, the mean is estimated as x and it can be shown that the standard deviation, for x greater than about 20, is $\sigma = \sqrt{x}$. Thus, for a single measurement, the reported value is $x \pm \sigma$. If a Gaussian distribution can approximate the data, then σ has a specific meaning, namely, there is a 68.3% probability that the next observed measurement will have a value that falls within the range $x \pm \sigma$. Table 2 shows the relationship between the number of radiation induced counts recorded and the percent standard deviation. For example, a standard error of one percent or less would require recording at least 10,000 counts.

Frequently, more than one measurement is recorded. If it is assumed the radiation source has constant activity, estimates of the mean and standard deviation can be obtained directly from the N measured values, $x_1, x_2, \ldots, x_N$. The experimental mean is the average value of the counts

$$\overline{x} = \frac{1}{N}\sum_{i=1}^{N} x_i. \tag{2}$$

Table 2. Standard deviation of count data measured with a radiation detector operating in pulse mode.

Observed Total Counts	% Standard Deviation (1σ error)
100	10%
400	5%
1100	3%
2500	2%
10000	1%

Table 3. Probability interval relative to the number of standard deviations based on the Gaussian distribution.

Number of Standard Deviations ($k\sigma$)	Probability Event is Observed within $\pm k\sigma$
0.67σ	0.500
1.00σ	0.683
1.65σ	0.900
1.96σ	0.950
3.00σ	0.997

Because $\sigma_i^2 = x_i$, the total variance for a series of measurements is

$$\sigma_{SUM}^2 = \sum_{i=1}^{N} x_i = \overline{x}N. \tag{3}$$

For a series of N like measurements, assuming that the activity of the radioactive source remains fairly constant during the measurement series, it can be shown with Eqs. (2) and (3) that the standard deviation of $\overline{x}$ is

$$\sigma_{\overline{x}} = \frac{\sqrt{\sigma_{SUM}^2}}{N} = \frac{\sqrt{\overline{x}N}}{N} = \sqrt{\frac{\overline{x}}{N}}. \tag{4}$$

If another series of N measurements were to be taken, a new average value for $\overline{x}$ would be found, yet there would be a 68.3% chance that the new average would fall within the interval ranging from $\overline{x} - \sigma_{\overline{x}}$ and $\overline{x} + \sigma_{\overline{x}}$. The result of N measurements is reported as

$$\overline{x} \pm \sigma_{\overline{x}} = \overline{x} \pm \sqrt{\frac{\overline{x}}{N}}. \tag{5}$$

Uncertainties are not always reported as one standard deviation. Sometimes a larger uncertainty is reported in order to increase the probability that the mean is included within the range between $x - k\sigma$ and $x + k\sigma$. As shown in Table 3, if the error is reported as one standard deviation, the probability is 68.3%. However for an error range of $x - 1.65\sigma$ to $x + 1.65\sigma$ the probability increases to 90%. This would be reported as the 90% *confidence interval*. However, the convention is to report errors as one standard deviation.

The Gaussian gamma-ray peak shape arises from the statistical fluctuations in the number of information (charge) carriers excited per monoenergetic gamma-ray interaction event. Typically the resolution of the gamma-ray peak from the detector is quoted as a function of the peak's *full width at half the maximum* value (FWHM), which for a Gaussian distribution is 2.355σ, where σ is in units of energy. In terms of percent, the *energy resolution* of the spectrometer is calculated by dividing 235.5σ by the gamma-ray energy.

7.3 Dead Time

All radiation detection systems operating in pulse mode have a limit on the maximum rate at which data can be recorded. The limiting component may be either the time response of the radiation detector such as that for a GM counter, or may be the resolving capability of the electronics. The true counting rate (n) for a detector with zero dead time losses is related to the recorded counting rate (m) for a detector with significant dead time losses by

$$n = \frac{m}{1 - m\tau}, \tag{6}$$

where τ is the dead time of the detector. Note that the term $m\tau$ is the fraction of the time that the detector is unable to respond to additional ionization in the active volume of the detector. When designing an experiment, it is advisable to keep these losses to a minimum. If possible, this means that $m\tau$ should be less than 0.05. For example, for a GM counter with a typical dead time of $\tau = 100$ μs, the maximum count rate would be 500 counts/s.

8 Summary

Since the discovery of x radiation by Röntgen in 1895, radiation detectors have undergone a variety of changes and improvements. These improvements include the changes from the initial use of scintillation phosphors such as $BaPt(CN)_4$ to present-day bright scintillation spectrometers, the first Geiger counters described in 1908 to present-day multi-wire proportional counters, the first semiconductor conduction counters as described in 1941 and 1945 to present-day single-carrier compound semiconductor designs and arrays (see McGregor and Shultis 2020). Usually progress with radiation detector development was slow with long periods of small incremental improvements. At times a single important innovation would bring about a grand improvement in radiation detector development, for example, the photomultiplier tube that was commercially introduced in 1941 is a fundamental component of modern scintillation spectrometers.

Such incremental development of radiation sensors punctuated by the introduction of novel new technology can be expected to continue. The vibrant surge in the development of radiation detectors and associated detector materials seen over the past 20 years resulted largely from new government programs and sponsorships such as, in the U.S., the 2002 Homeland Security Act, which had an avalanche effect on other governmental agencies to also focus on radiation sensors. As these programs now wane, radiation sensor development will still be driven by new applications in basic research (such as high energy and space physics), specialized commercial applications (such as medical imaging), military applications, and, indeed, by scientific curiosity. The universe is awash with radiation of different types and new radiation sensors will be needed for us to understand better the greater environment in which we exist.

Bibliography

Apfel RE (1979) The Superheated Drop Detector. *Nucl. Instrum. Meth.* 162: 603-608.

Autagawa W, Zanio K, and Mayer JW (1967) CdTe as a Gamma Detector. *Nucl. Instrum. Meth.* 55: 383-385.

Austin L and Starke H (1902) Ueber die Reflexion der Kathodenstrahlen und eine damit verbundene neue Erscheinung secundrer Emission. *Ann. Physik* 314: 271-292.

Becquerel AH (1900) Déviation du Rayonnement du Radium dans un Champ Électrique, *Compte Rendus*, 130: 809-815.

Bertolini G and Coche A (1968) *Semiconductor Detectors*. New York: Wiley.

Bevington PR and Robinson DK (1992) *Data Reduction and Error Analysis for the Physical Sciences*, 2nd Ed. New York: McGraw-Hill.

Birks JB (1964) *The Theory and Practice of Scintillation Counting*. Oxford: Pergamon Press.

Bøtter-Jensen L, McKeever SWS, and Winkel AG (2003) *Optically Stimulated Luminescence Dosimetry*. Amsterdam: Elsevier.

Broser von I and Kallman H (1947a) "Uber die Anregung von Leuchtstoffen Durch Schnelle Korpuskularteilchen I. *Z. Naturforschung* 2a: 439-440.

Broser von I and Kallman H (1947b) Über den Elementarprozess der Lichtanregung in Leuchtstoffen Durch Alpha-Teilchen Schnelle Elektronen und Gamma-Quanten II. *Z. Naturforschung* 2a: 642-650.

Brown WL, Higinbotham AH, and Miller GL (Eds.) (1969) *Semiconductor Nuclear-Particle Detectors and Circuits*, Pub. 1593. Washington: National Academy of Sciences.

Butler JF, Lingren CL, and Doty FP (1992) $Cd_{1-x}Zn_xTe$ Gamma Ray Detectors. *IEEE Trans. Nucl. Sci.* 39: 605-609.

Cameron JR, Suntharalingam N, and Kenney GN (1968) *Thermoluminescent Dosimetry*. Madison: U. Wisconsin

Press.
Cember H (1983) *Introduction to Health Physics*, 2nd Ed. New York: Pergamon Press.
Chadwick J (1932) Existence of a Neutron. *Proc. Royal Society A* 136: 692-708.
Cova S, Lacaita A, Ghioni M, Ripamonti G, and Louis TA (1989) 20-ps Timing Resolution with Single-Photon Avalanche Diodes. *Rev. Sci. Instrum.* 60: 1104-1110.
Dearnaley G and Northrop DC (1966) *Semiconductor Counters for Nuclear Radiations*, 2nd Ed. New York: Wiley.
Donati S (2000) *Photodetectors*. Upper Saddle River: Prentice Hall.
Doty FP, Lingren CL, and Butler JF (1992) $Cd_{1-x}Zn_xTe$ Gamma-Ray Detectors. *IEEE Trans. Nucl. Sci.* NS-39: 605-609.
Engstrom RW, and unknown others (1980) *Photomultiplier Handbook*. Lancaster: Burle Technologies, Inc.
Enss C, (Ed.) (2005) *Cryogenic Particle Detectors* vol. 99 in *Topics in Applied Physics*. New York: Springer.
Eichholz GG and Poston JW (1979) *Principles of Radiation Detection*. Ann Arbor: Ann Arbor Science.
Evans RD (1955) *The Atomic Nucleus*. New York: McGraw-Hill.
Geiger H and Müller W (1928) Das Elektronenzählrohr. *Phys. Zeitschrift* 29: 839-841.
Glaser DA (1952) Some Effects of Ionizing Radiation on the Formation of Bubbles in Liquids. *Phys. Rev.* 87:665.
Goldstein JI, Newbury DE, Echlin P, Joy DC, Fiori C, and Lifshin E (1981) *Scanning Electron Microscopy and X-Ray Microanalysis*. New York: Plenum.
Grosshoeg G (1979) Neutron Ionization Chambers. *Nucl. Instrum. Meth.* 162: 125-160.
Haitz RH (1961) Model of the Electrical Behavior of a Microplasma, *J. Appl. Phys.* 35: 1370-1376.
Hofstadter R (1949) The Detection of Gamma-rays with Thallium-Activated Sodium Iodide Crystals. *Phys. Rev.* 75: 796-810.
Horrocks DL and Peng CT (1971) *Organic Scintillators and Liquid Scintillation Counting*. New York: Academic Press.
Kaplan I (1962) *Nuclear Physics*. Reading: Addison-Wesley.
Korff SA (1946) *Electron and Nuclear Counters*. New York: Van Nostrand.
Lecoq P, Annenkov A, Gektin A, Korzhik M, and Pedrini C (2006) *Inorganic Scintillators for Detector Systems*. Berlin: Springer.
Liebson S (1947) The Discharge Mechanism of Self-Quenching Geiger-Mueller Counters. *Phys. Rev.* 72: 602-608.
Liebson S and Friedman H (1948) Self-Quenching Halogen-Filled Counters. *Rev. Sci. Instrum.* 19:303-306.
Malm HL (1972) A Mercuric Iodide Gamma-Ray Spectrometer. *IEEE Trans. Nucl. Sci.* NS-19: 293-265.
Mayer JW (1967) Evaluation of CdTe by Nuclear Particle Measurements. *J. Appl. Phys.* 38: 296-301.
McGregor DS (2018) Materials for Gamma-Ray Spectrometers: Inorganic Scintillators. *Ann. Rev. Mater. Res.* 48: 13.1-13.33.
McGregor DS and Hermon H (1997) Room Temperature Compound Semiconductor Radiation Detectors. *Nucl. Instrum. Meth.* A395: 101-124.
McGregor DS and Shultis JK (2020) *Radiation Detection: Concepts, Methods, and Devices*. Boca Raton: CRC Press.
McIntyre RJ (1961) Theory of Microplasma Instability of Silicon. *J. Appl. Phys.* 32: 983-995.
McKeever SWS (1985) *Thermoluminescence of Solids*. Cambridge: Cambridge Univ. Press.
NCRP (1985) *A Handbook of Radioactivity Measurements Procedures*, 2nd Ed. NCRP Report No. 58, Bethesda, MD: National Council on Radiation Protection and Measurements.
Owens A (2012) *Compound Semiconductor Radiation Detectors*. Boca Raton: CRC Press.
Owens A (2019) *Semiconductor Radiation Detectors*. Boca Raton: CRC Press.
Pell EM (1960) Ion Drift in an n-p Junction. *J. Appl. Physics* 31: 291-302.
Price WJ (1964) *Nuclear Radiation Detection*, 2nd. Ed. New York: McGraw-Hill.
Renker D (2006) Geiger-Mode Avalanche Photodiodes, History, Properties and Problems. *Nucl. Instrum. Meth.* A567: 48-56.
Ridley BK (1982) *Quantum Processes in Semiconductors*. Oxford: Clarendon Press.
Rodnyi PA (1997) *Physical Processes in Inorganic Scintillators*. Boca Raton: CRC Press.
Röntgen W (1895) Ueber eine neue Art von Strahlen. Vorläufige Mitteilung, *Aus den Sitzungsberichten der Würzburger Physik.-medic* Gesellschaft Würzburg, 137-147.
Röntgen W (1896) Eine neue Art von Strahlen. 2. Mitteilung, *Aus den Sitzungsberichten der Würzburger Physik.-*

medic. Gesellschaft Würzburg, 11-17.
Röntgen WC and Joffé A (1913) Über die Elektrizitätsleitung in einigen Kristallen und über den Einfluß der Bestrahlung darauf. *Ann. der Phys.*, 41: 449-498.
Rutherford E (1899) VIII. Uranium Radiation and the Electrical Conduction Produced by It. *Philosophical Magazine* 47(284): 109-163.
Rutherford E and Geiger H (1908) An Electrical Method of Counting the Number of α-Particles from Radio-Active Substances. *Proc. Royal Soc. London A* 81: 141-161.
Sauli F (2014) *Gaseous Radiation Detectors*. Cambridge: Cambridge University Press.
Sitar B, Merson GI, Chechin VA, Budagov YuA (1993) *Ionization Measurements in High Energy Physics*. Berlin: Springer.
Shafroth SM Ed. (1967) *Scintillation Spectroscopy of Gamma Radiation*. London: Gordon and Breach.
Shultis JK and Faw RE (2000) *Radiation Shielding*. La Grange Park: American Nuclear Society.
Slepian J (1923) U.S. Patent 1,450,265.
Stetter G (1941) Durch Korpuskularstrahlen in Kristallen Hervorgerufene Elektronenleitung. *Verh. d. D. Phys. Ges.*, 22: 13-14.
Sze SM (1981) *Physics of Semiconductor Devices*, 2nd Ed. New York: Wiley.
Thomson JJ (1897) Cathode Rays. *Phil. Mag.* 44: 293-316.
Tsoulfanidis N and Landsberger S (2015) *Measurement and Detection of Radiation*, 4th Ed. Boca Raton: CRC Press.
Van Heerden PJ (1945) *The Crystal Counter, A New Instrument in Nuclear Physics*. Amsterdam: Noorde-Hollandsche Uitgevers-Mij.
Villard P (1900a) Sur la Réflexion et la Réfraction des Rayons Cathodiques et des Rayons Déviables du Radium. *Comptes Rendus* 130: 1010-1012.
Villard P (1900b) Sur le Rayonnement du Radium. *Comptes Rendus* 130: 1178-1179.
Wilkinson DH (1950) *Ionization Chambers and Counters*. Cambridge: Cambridge University Press.
Willig WR (1971) Mercury Iodide as a Gamma Spectrometer. *Nucl. Instrum. Meth.* 96:615-616.
Wilson CTR (1911) On a Method of Making Visible the Paths of Ionising Particles Through a Gas. *Proc. R. Soc. Lond. A* 85: 285-288.
Wilson CTR (1912) On an Expansion Apparatus for Making Visible the Tracks of Ionising Particles in Gases and Some Results Obtained by Its Use. *Proc. R. Soc. Lond. A* 87: 277-292.
Yen WM, Shionoya S, and Yamamoto H (2007) *Fundamentals of Phosphors*. Boca Raton: CRC Press.
Yukihara EG and McKeever SWS (2011) *Optically Stimulated Luminescence Fundamentals and Applications*. New York: Wiley.